Interfacial Electrodeposition of Silver

L. Zeiri, O. Younes, and S. Efrima*

Department Of Chemistry, Ben Gurion University, POB 653, Beer-Sheva, Israel, 84105

M. Deutsch

Department of Physics, Bar Ilan University, Ramat Gan, Israel 52900

Received: June 2, 1997; In Final Form: August 11, 1997[⊗]

A systematic study of silver ion electrodeposition at the water/air and water/dichloromethane interfaces, under potentiostatic control, is presented. We study the morphology of the deposits and their growth rate, as a function of several important physical and chemical parameters, namely, the electric voltage, the silver ion concentration, the conductivity, the viscosity, and the presence of a surfactant and an organic anionic additive known to associate with silver. The results are discussed in terms of a generalized Wagner number, which is shown to correlate well with the observations and to be a highly reliable predictive tool for the morphologies.

Introduction

Metal electrodeposition is of great importance, both for the basic science involved in this process and for its major technological applications in electroplating, metal electrorefining and electrowinning, and electroforming as well as its relevance to the inverse process of electromachining.[1]

Two-dimensional metal electrodeposition has been used recently as a convenient system to study the formation and growth of macroscopic patterns and their relationship to the underlying microscopic mechanisms.[2] Zinc deposition was used in most of the studies,[2a−c] a few investigated copper,[2d,e] and only a few address silver electrodepostion.[3]

Most of the studies used a thin cell geometry, where the deposit was confined to the narrow gap between two plates.[2] Only a few studies investigated electrodeposition at the surface of water or at the water/organic liquid interface,[2c] where no rigidly fixed space limitations are imposed on the process. At the interface a richer array of shapes and patterns of growth is available, as compared to the thin cell configuration, including growth into the third dimension. Throughout this report we address electrodeposition, where an electrochemical process occurs at the metal−solution interface, and the electrodepsit may (or may not) be constrained to form along the liquid surface or interface.

In contrast to electrodeposition in the bulk of a homogeneous liquid, electrodeposition at the interface between two imiscible liquids (water/organic) provides for the introduction of an additional important system parameter, the nature of the organic subphase. Recently we showed that the characteristics of the electrodeposit depend strongly on the subphase, in a way that reflected the wetting properties at the interface.[4] In another study we discussed the effect of poisoning ions on the morphology of the deposit and demonstrated a drastic transition from a 2D to a 3D pattern of growth (the Hecker effect).[5]

Here we present a systematic study of the electrodeposition of silver at the water/air and water/dichloromethane (DCM) interfaces under potentiostatic control. These particular interfaces were chosen since they have very different wetting characteristics,[4] exhibit different relative rates for the various processes controlling the growth, and yield different deposit topologies, despite having one phase in common. We study the deposit's morphology and the growth process as a function of the main experimental parameters: the electric potential, the concentration of the silver ions, and the conductivity of the solution. We also study the effect of the viscosity and the presence of additives known to affect the surface tension and to associate with silver ions and silver surfaces. We monitor the morphology of the deposits, the rate of their growth, and the electrical currents. We discuss the behavior in terms of a generalized Wagner number,[6] which is a dimensionless quantity determined by the intrinsic rates of charge transport across the solution, the mass transport to the growing electrode, and the charge transfer across the electrode/solution interface.

Experiment

A three-electrode, potentiostatic (EG&G PAR 173) electrochemical setup is employed. The electrodeposition is carried out in a circular cell of radius 3.3 cm. The silver wire working electrode is placed at the center of the cell, with its tip just touching the aqueous solution/air or the water/dichloromethane interface. The counter electrode is an aluminum strip placed around the inner circumference of the cell. Aluminum was used for convenience. Tests show that it yields the same morphologies and growth characteristics as those obtained with a silver anode. The reference is a saturated calomel electrode separated from the solution with a homemade luggin capillary.

A Sony SSC-M370CE video camera and a Sony SLV383 VCR are used to monitor and record the progress of the electrodeposition. A framegrabber, Data Translation 3955, and the Global Lab image package (Data Translation) are used to import the images into a computer and for subsequent analysis. The time-dependent electric current is measured by a data acquisition Advantech 812PG board installed in a 286 IBM PC.

Our standard conditions throughout these measurements are a solution containing 0.05 M silver nitrate (Merck), 0.1% anisic acid (Aldrich Chemicals Inc.) and 0.03% FC143 (a 3M perfluroalkyl anionic surfactant, consisting predominately of perfluorooctanoic ammonium salt). The solution is made basic by the addition of ammonia until the silver oxide just dissolves (pH ∼9). NH_4NO_3 is used as an inert electrolyte to control the conductivity of the solution. The growth rates and shapes are affected only marginally by the addition of the small amounts of anisic acid and/or a surfactant that were added to the solution.

[⊗] Abstract published in *Advance ACS Abstracts,* October 1, 1997.

S1089-5647(97)01772-0 CCC: $14.00

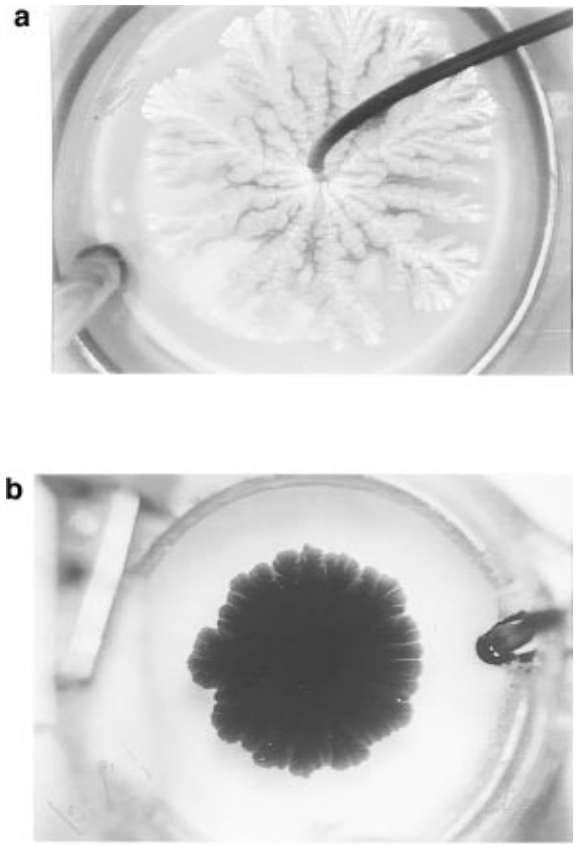

Figure 1. Silver electrodeposits at standard conditions: (a) water/air, (b) water/ dichloromethane. Standard conditions: 0.05 N $AgNO_3$ amoniacal solution at a cathodic voltage of 5 V.

However, without these additives a finer alignment of the cathode tip at the interface is needed to obtain reproducible results.[4,5]

The viscosity is altered by adding ethylene glycol to the aqueous solution. All materials are used as purchased. Water is Barnsted E-Pure quality, with a specific resistivity of ~18 MΩ cm.

Results

A. Introduction. Figure 1 shows the electrodeposit of silver under our standard conditions, for both interfaces studied, i.e., using the standard composition of the aqueous phase, as given in the Experiment Section, and applying −5 V. This serves as a reference point for all the other experiments, when the various experimental parameters are changed. At the water/air interface the silver-colored deposit is ramified, with rather thick branches. Delicate veins are clearly seen running along the branches. At the water/DCM interface a more compact black "flower" is obtained with a rough perimeter. In both cases the typical growth velocity is 0.1 ± 0.01 cm/s. The thickness of the deposit at the water/air interface is estimated as ~20 nm at the edge of the deposit and ~80 nm at its center. It is determined by three different and independent methods: electrical conductivity of the deposit, its weight, and light transmission through it. Similar values were obtained for the water/DCM inteface, although the surface of the deposit is rougher. This is a clear case of a quasi-two-dimensional growth, with an aspect ratio of over 10^6.

In general, the morphological changes induced by varying the various control parameters are more pronounced at the water/air interface than those observed at the water/DCM interface. Specifically, the variety of deposit shapes is usually larger, and transitions from 2D (silvery) to 3D (black) deposits are easier to observe. Deposits at the water/DCM interface usually require a more detailed quantitative analysis in order to reveal the trends.

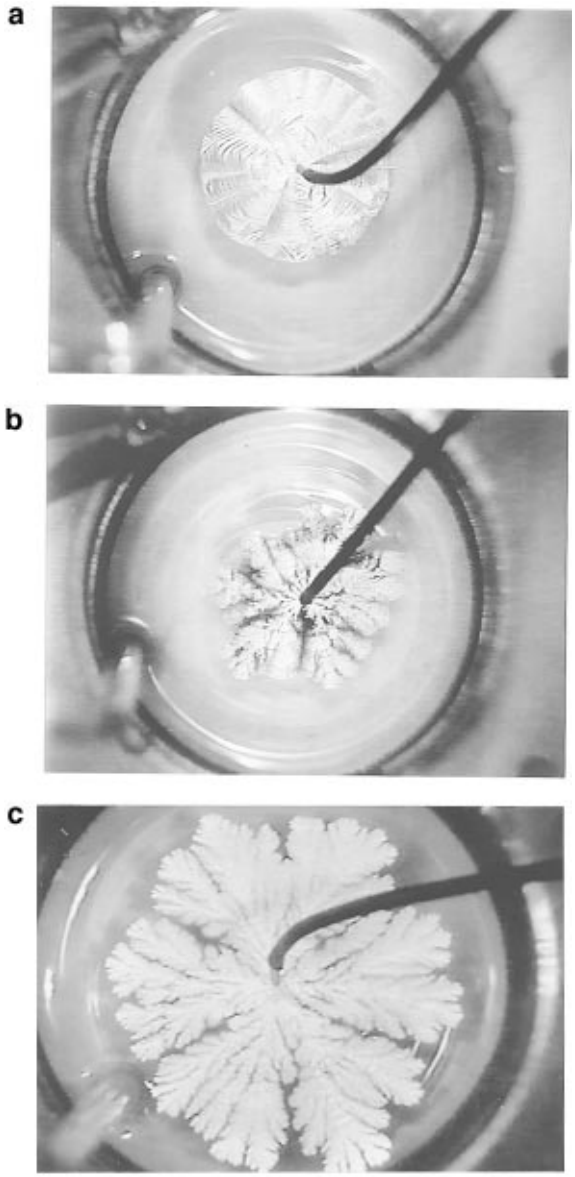

Figure 2. Influence of the voltage on the morphology of silver electrodeposits at the water/air surface: (a) 2 V, (b) 4 V, (c) 6 V.

We now discuss in turn the results obtained for the dependence of the morphology and growth process on each of the control parameters.

B. Depositing Voltage. The voltage dependence at the standard composition is measured at 1 V intervals in the range −2 to −7 V. Selected frames for the water/air interface are shown in Figure 2.

At the water/air interface the morphology changes from highly compact, disklike deposits at low voltages (1−3 V), to finely branched, ramified patterns at higher voltages (4−5 V), which become more compact again at 6−7 V, when hydrogen evolution becomes significant**.** The dependence on the applied voltage is also reflected in the electric currents, as shown in Figure 3. The current exhibits an onset with a steep rise for most of the potentials above about cathodic ~3 V. The higher the potential, the steeper the increase in the electric current**.** The inset in Figure 3 shows the evolution of the electric currents as a function of time, normalized to the total time required for the deposit to reach the edge of the cell at each potential. Roughly, all the curves coincide, although the initial slopes are usually somewhat larger for the higher potentials. The total time required for the deposit to reach the anode at the perimeter of the cell depends on the electric potential. This can be seen in Figure 3 from the upper limit of the time for each potential.

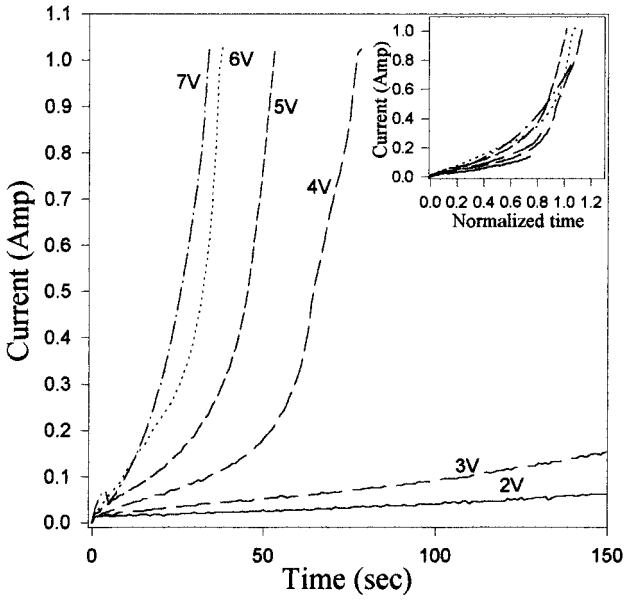

Figure 3. Electric current vs time for silver ion deposition at the water/air surface. Standard conditions are used (see text). Inset: current vs normalized time. The normalization is with respect to the total time required to form a deposit across the cell in each case.

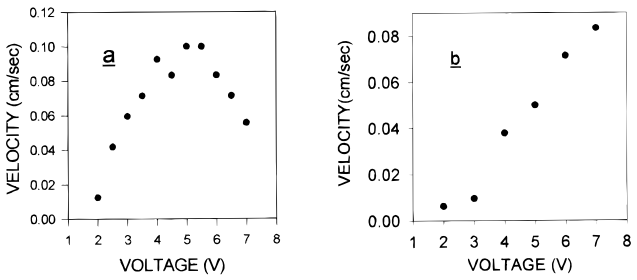

Figure 4. Dependence of the velocity of growth on the voltage: (a) for water/dichloromethane; (b) water/air. Depositions at standard conditions.

At the water/DCM interface the morphological changes induced by a variation of the depositing volatge are smaller. The shapes are rather compact, and only the edges show some roughness. As shown below, even a quantitative analysis fails to detect any clear trend. Typically, the average, minimal, and maximal radii of the deposit grow linearly with time, except, perhaps, at the very beginning of the deposition.

The growth rates, as obtained from the slopes of radii vs time curves, are ploted against voltage in Figure 4, for the water/DCM (Figure 4a) and the water/air (Figure 4b) systems. For water/DCM an increase of the growth rate is observed up to a maximum at about 6 V, followed by a decrease at higher volatges. The decrease is strongly correlated with the vigorous hydrogen evolution at these voltages. At the water/air interface (Figure 4b) the rate increases monotonically, even above theses voltage.

C. Ionic Strength. The ionic strength of the solution, which dominates the conductivity, is varied by adding NH_4NO_3, an inert electrolyte, to a standard solution. The effect of increasing the ionic strength is similar for both interfaces. The deposition is slowed, and the shapes become more compact. At higher ionic strengths, >0.1 M, hydrogen release is observed and becomes more dominant with increasing ionic strength. Concomitantly, the deposition becomes increasingly slower and more three-dimensional in nature. The effect on the morphology in the water/air surface is demonstrated by comparing Figure 1a for 0.054 M and Figure 5 for 0.154, 0.554, and 1.354 M, where transitions between silvery 2D deposition to black 3D deposition are apparent. Similar behavior is observed for the

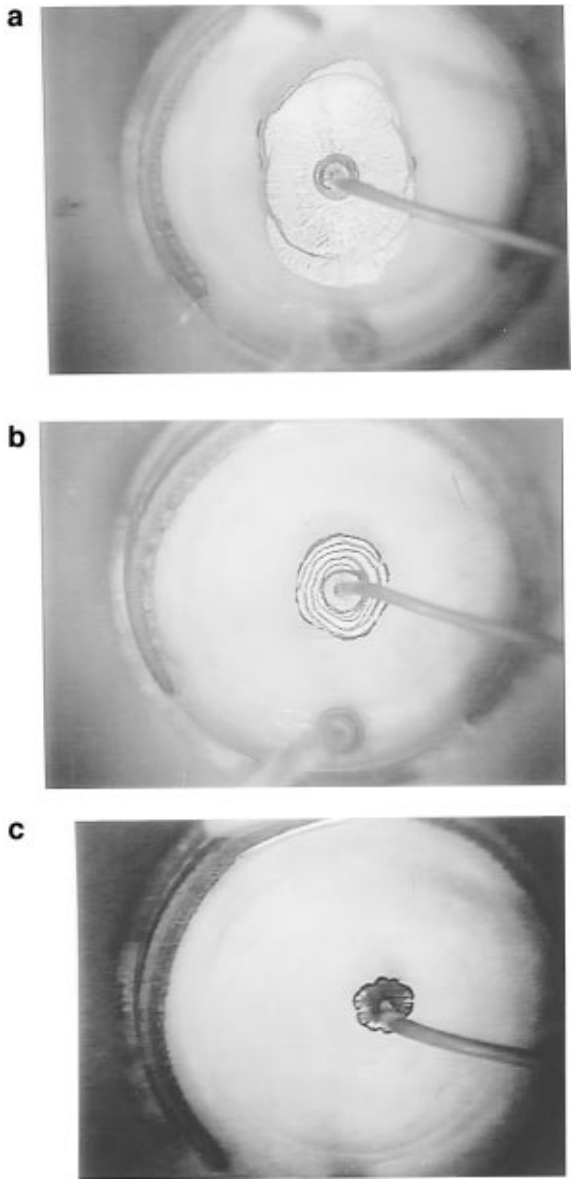

Figure 5. Effect of the ionic strength on the morphology of the deposits at the water/air surface. The ionic strengths are (a) 0.154 M, (b) 0.554 M, (c) 1.354 M. The voltage is −5 V; standard composition is used (except for the ionic strength).

DCM interface, where increasingly more compact and slower deposits are obtained as the ionic strength increases.

D. Combined Voltage and Ionic Strength Variations. A simultaneous variation of the two control parameters, the electric potential and the ionic strength, produces a variety of effects. Keeping the ionic strength constant and varying the voltage changes the shapes from ramified to compact with an increase in the growth rate. When both the voltage and ionic strengths are high, $V > \sim 5\ V$ and ionic stength > ~ 1 M, a large increase in the current is obtained and the potentiostat reaches saturation conditions, which, in turn, results in very small deposits.

The deposits at the water/air interface, at an ionic strength ≥ 0.154 M, usually tend to be ramified or flat disks at low voltages (Figure 6a) and three-dimensional at high voltages (Figure 6c). At intermediate potentials a banded structure of alternating 2D and 3D rings appears (Figure 6b). This novel oscillatory behavior is discussed in detail elsewhere.[7] This behavior is observed in Figure 5b, where formation of ring structure is apparent. As the ionic strength increases, the 3D morphology sets in at lower potentials, the ring formation is shifted to even lower voltages, and the 2D disk structures may not appear at all.

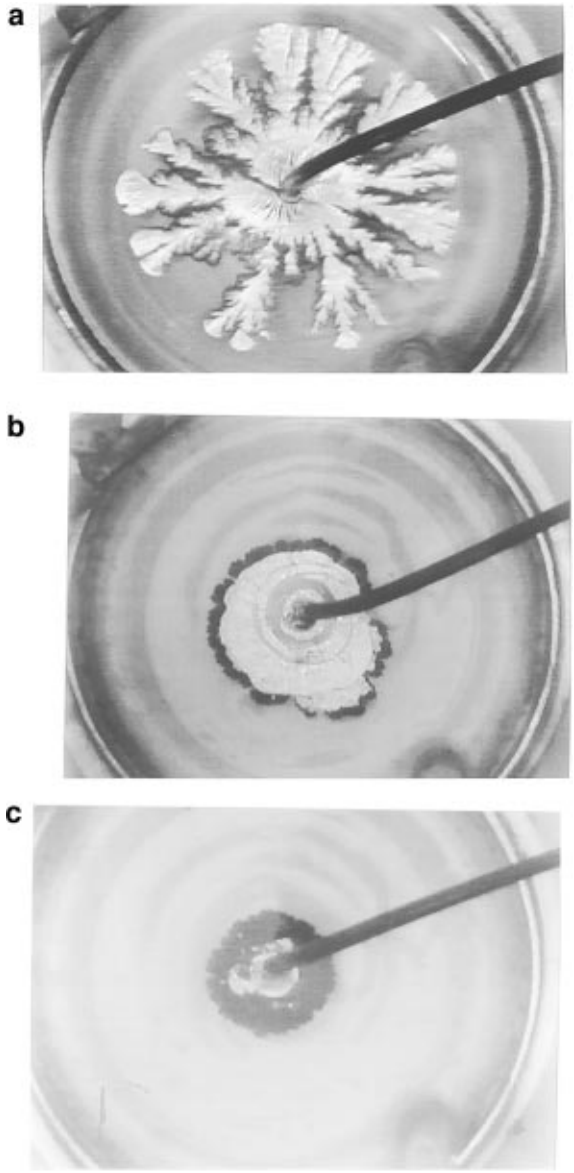

Figure 6. Effect of the voltage on the morphology of electrodeposits at the water/air surface: (a) $I = 0.154$ M, $V = 3$ V; (b) $I = 0.554$ M, $V = 4$ V; (c) $I = 0.554$ M, $V = 6$ V.

The voltage variations affect the growth rates and currents as well. At the intermediate ionic strengths the current vs time curves show a maximum at ~ -5 V, and they decline at both sides of this potential.

Similar trends, i.e., slower deposition and more compact forms with increasing ionic strengths, are obtained also at the water/DCM interfaces. An analysis of the growth rates at various silver ion concentrations and ionic strengths is shown in Figure 7. At high ionic strengths, above ~ 1 M, a vigorous hydrogen release is observed, which perceptibly perturbs the deposition process.

A morphology diagram, depicting the various patterns observed and their ranges of existence in the ionic strength−depositing voltage plane, is shown in Figure 8 for the air/water interface at a 0.05 M silver concentration. In general, low ionic strengths favor ramified, 2D structures. High voltages and ionic strengths are associated with compact, 3D deposits. Rings, alternating 2D and 3D deposits, appear over a wide range of experimental conditions in a broad band separating these two regions. The region denoted "mixed" is characterized by the formation of rings in the initial stages of the deposition and a transition to a 2D compact structure as it progresses. As already stated, the variations in the morphology of the deposits at the water/DCM interface were much smaller, and only compact patterns are observed, with varying degrees of edge roughness.

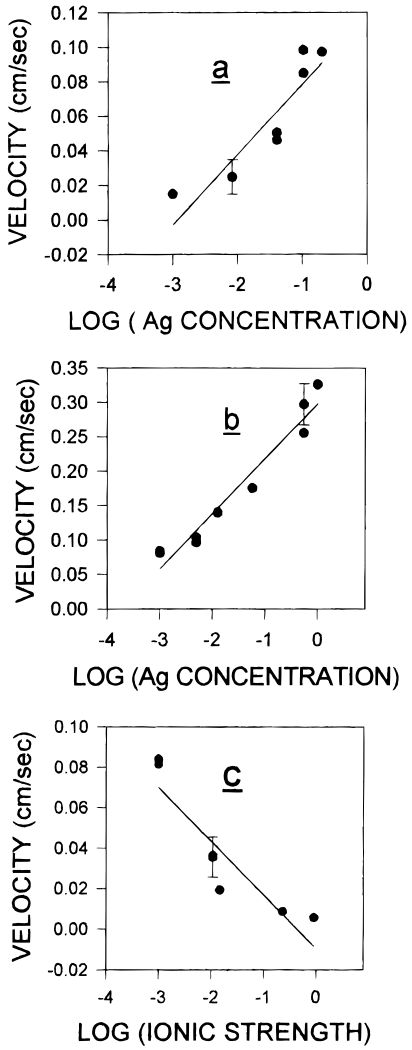

Figure 7. Dependence of the growth velocity on the ionic strength and on the silver ion concentration for electrodeposition at the water/dichloromethane interface. Voltage is −5 V. (a) Ag ion concentration changes with the ionic strength fixed at $I = 0.5$ M. (b) Ag ion concentration and the ionic strength change. (c) Ionic strength changes at constant Ag ion concentration of 0.05 M.

E. Silver Concentration. Varying the concentration of the silver ions, with the ionic strength changing accordingly, produces the deposits shown in Figure 9 for the water/air interface and in Figure 10 for dichloromethane. In both systems very ramified structures form when the silver ion concentration is low (below ~ 0.005 M) or high (above ~ 0.1 M). At high concentrations the deposition is very fast, e.g. about 5 s for a maximally developed deposit at 1 M, and exhibits fine branches. At very low concentrations the deposition is very slow, e.g. 350 s for the maximal size deposit at 0.0005 M, and the branches of the deposit tend to broaden with time. At intermediate silver concentrations more compact structures appear, although at the water/air interface residual branching is still observed as veins decorating the deposit. The electric currents increase steadily when the concentration increases. The rate of growth increases logarithmically with the silver concentration, as shown in Figure 7.

Similar phenomena are observed when the silver concentration is varied while the ionic strength is kept constant, using NH_4NO_3. An example is shown in Figure 11 for the water/air interface and a constant ionic strength of 1 M. As can be seen, the morphology becomes more branched for the higher silver

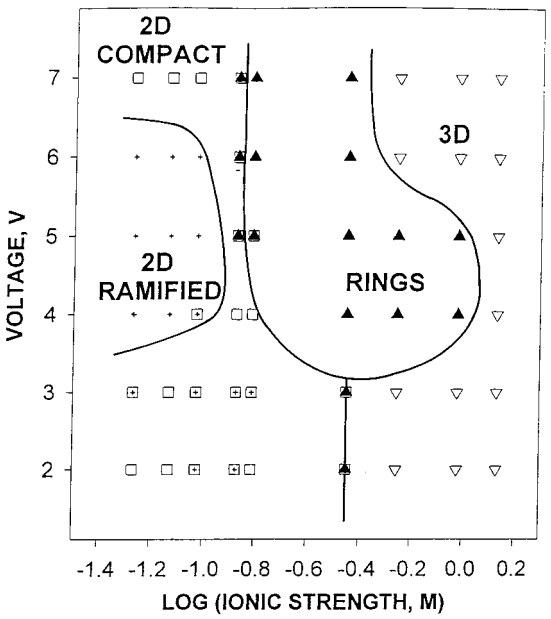

Figure 8. Shape diagram for silver electrodeposition at the water/air surface. The silver ion concentration is 0.05 M.

concentrations. It is interesting to note that the increasing silver ion concentration totally cancels the deleterious effect of the ionic strength (when acting alone) on the rates, shown in Figure 7a.

F. Viscosity. Increasing the viscosity in the range 1 to ~5 cP slows down the process dramatically, as shown in Figure 12a, and somewhat increases the ramification of the deposit, at both interfaces studied. The growth rates scale inversly with the viscosity. Figure 12b shows the dependence of the current on the normalized growth time, for various concentrations of ethylene glycol. The normalization is carried out with respect to the time required for the deposit to reach the edge of the cell. By and large, the normalized behavior of the currents at different viscosities is similar, which is another manifestation of the scaling with viscosity.

G. Effect of Additives. We have used two additives: a surfactant and anisic acid. In Figure 2 of ref 4 the influence of the surfactant was shown. The surfactant tends to broaden the branches of the deposit. At excessively high surfactant concentrations, >1% (near its cmc), the deposit turns entirely compact, but remains two-dimensional. The deposition rate decreases by a factor of 10 at this surfactant concentration, and the deposit seems less smooth and with circular lines on it. However, at the relatively low surfactant concentrations used in the present study, we observe only a negligible effect of the surfactant on the deposit's shape and the growth rates. Although we could have done without the surfactant altogether, its presence facilitates the formation of the 2D deposition, as compared to 3D deposition. The anisic acid, too, has only a small effect on both the morphology and the shape. It seems to increase the smoothness of the deposit, as indicated by an increase in its reflectivity. At times, in its presence, transitions between silver and gold hues are observed in the deposit.

Discussion

A. Wagner Number. We propose to discuss the results of this study in terms of the generalized Wagner number.[6,8,9] The usual Wagner number is given by

$$W = R_f/R_s = \sigma_s/\sigma_f \quad (1)$$

Here R_f is the resistance of the Faraday reaction, R_s is the ohmic resistance of the solution across a characteristic distance of interest, l, and σ_s and σ_f are the reciprocals of the ohmic and Faradaic resistances, respectively ($\sigma = 1/R$).

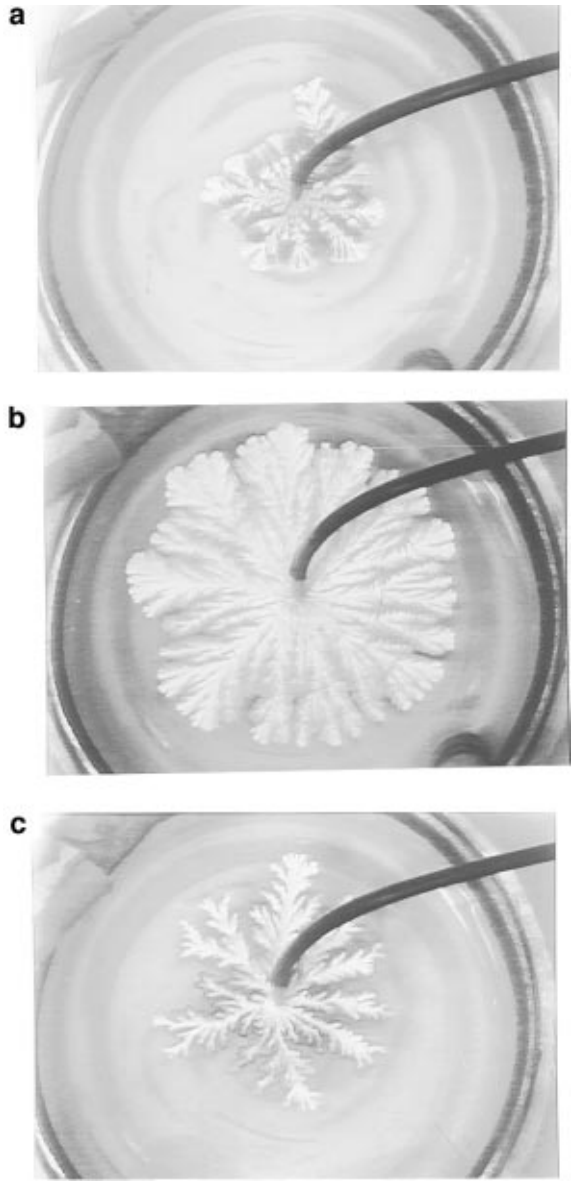

Figure 9. Electrodeposits at the water/air surface with varying silver ion concentrations. The toal ionic strength varies with the concentration. Silver concentrations: (a) 0.005 M; (b) 0.1 M; (c) 0.5 M.

A small Wagner number for a given deposition process means that the morphology is controlled by the differences in electrical resistance in the solution between various points on the growing cathode, separated by a distance l. Under these circumstances protrusions are amplified, instabilities set in, and the deposits tend to be ramified over length scales that give significant values of the ohmic resistance.

When the Wagner number is large, the current distribution is controlled by the electrodic charge-transfer act itself. The process tends to be rather slow, and the deposit turns out to be compact, utilizing most of the topological space in which it is embedded, with no preference for any particular direction.

The Wagner number has been discussed extensively in the past.[9] It was also realized that it can be generalized to include mass transport in addition to the current migration and the intrinsic electrodic elementary step. This approach was applied recently to interfacial electrodeposition.[10]

Very recently we derived a generalized form of the Wagner number which incorporates mass transport and IR corrections, in addition to the intrinsic electrochemical Faradaic resistance

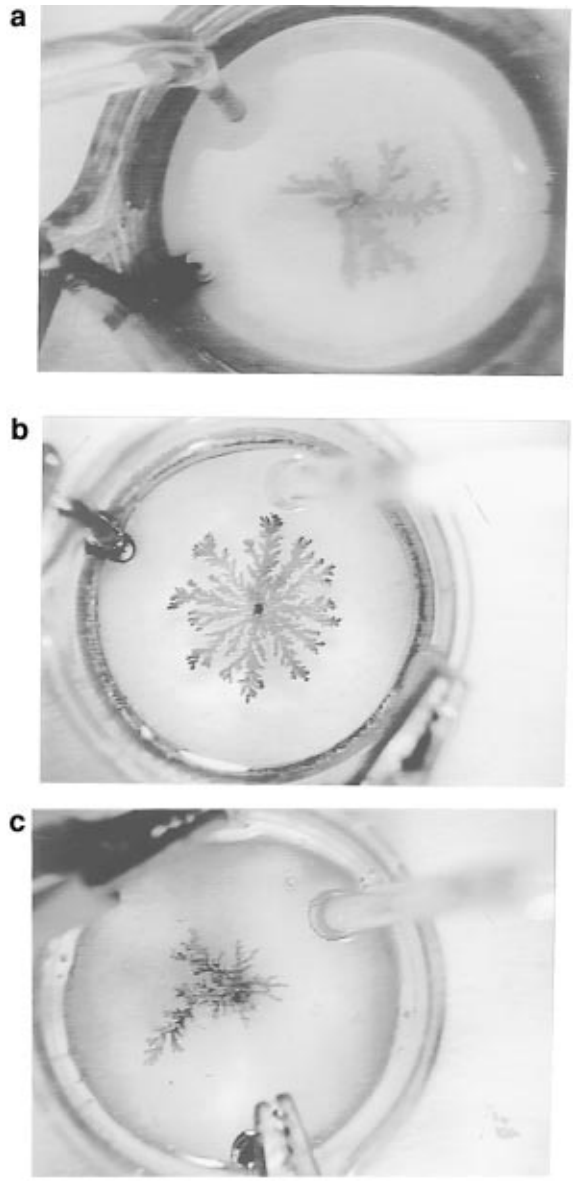

Figure 10. Electrodeposits at the water/dichloromethane interface with varying silver ion concentrations: (a) 0.0005 M; (b) 1.0 M; (c) 2.5 M. The total ionic strength varies with the concentration.

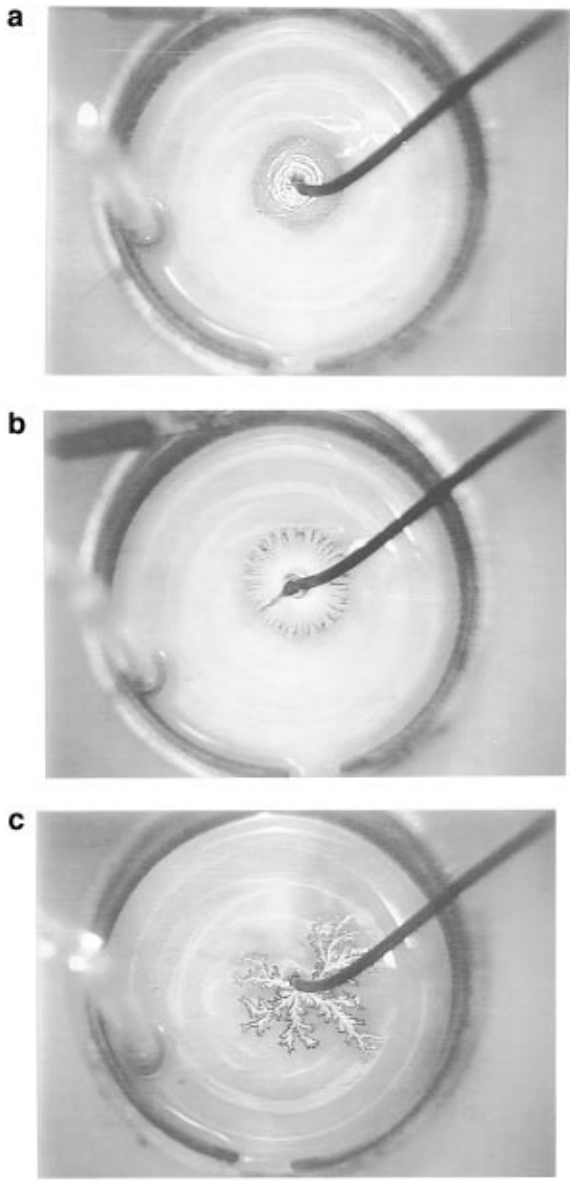

Figure 11. Silver electrodeposits at water/air surface with constant ionic strength of 1.0 M for various silver ion concentrations: (a) 0.1 M; (b) 0.5 M; (c) 1.0 M.

and the ohmic resistance across the solution.[6] We demonstrated its use for a rectangular configuration (parallel working and counter electrodes). Here we apply it to disk-shaped electrodes such as those obtained in the experiments described above. For simplicity, we assume throughout Tafel conditions, although our results can easily be generalized to the linear regime as well.

The generalized Wagner number is derived from the inverse of the relative difference in the current densities flowing at two points on the electrode at positions x and $x + l$:

$$W = \frac{i(x)}{i(x+l) - i(x)} \tag{2}$$

Here i(x) is the current density at a point x. For simplicity we avoid vector notation. Assuming the distance between the points to be small, a Taylor expansion up to the first derivative yields

$$W = \frac{i(x)}{(\partial i/\partial x)l} \tag{3}$$

In practice, l is the minimal spatial distance resolvable in the experiment. It is easy to see that when only Faradic and ohmic resistances are considered, the usual definition of eq 1 is recovered.

When the various effects co-occurring in our experiment are taken into account, this definition of the generalized Wagner number yields[6]

$$W = \frac{1}{l\{1 + [i_o/i_L(x)]\zeta(x)\}} \times \frac{\{1 + [i_o/i_L(x)]\zeta(x)\}^2 + (i_o/b)\zeta(x)\left[\left(\frac{RT}{nF}\right)\left(1 - \frac{i}{i_L}\right)^{-1}\left(\frac{1}{i_L}\right) + R_L(x)\right]}{(1/b)\left\{\left[\left(\frac{RT}{nF}\right)\left(1 - \frac{i}{i_L}\right)^{-1}\left(\frac{i}{i_L}\right) + bi_o/i_L(x)\zeta(x)\right]\frac{\partial \ln i_L}{\partial x} - i\frac{\partial R_L}{\partial x}\right\}} \tag{4}$$

with

$$\zeta(x) = \exp\{b^{-1}[\eta(x) - i(x)\, R_L(x)]\} \tag{5}$$

for the Tafel region. i_0 is the exchange current density, b is the Tafel slope (divided by 2.303), η is the overpotential set by the external device (e.g. by potentiostatic control, as done here), and R_L is the resistance between the reference electrode and the point x. i_L is the limiting current density, usually taken to be of the form

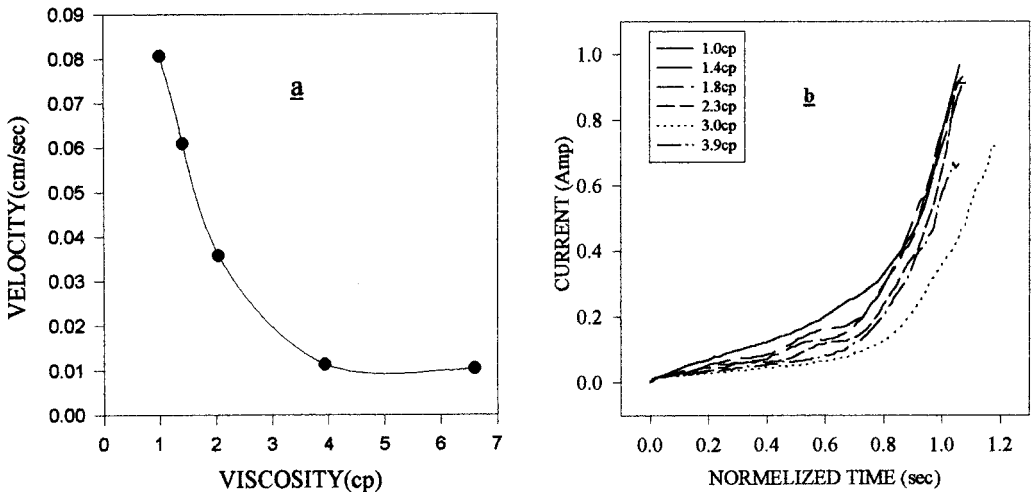

Figure 12. Deposition as a function of the viscosity of the aqueous subphase. (a) Rate of growth of silver electrodeposits at the water/dichloromethane interface. (b) Electric currents for silver electrodeposition at the water/air surface. Voltage −5 V, silver ion concentration 0.05 M.

$$i_L = nFDC^\circ/\delta \tag{6}$$

where n is the number of electrons required to neutralize the metal ion, F is the faraday constant, D is the diffusion constant, C° is the concentration of the reactant in the bulk of the solution, and δ is the width of the Nernst diffusion layer. The dependence of the limiting current on the position x comes in through the dependence of δ on x. Equation 4 includes activation, migration, diffusion, and the IR correction. Convection and stirring effects can also be included. Further details are given in ref 6.

The spatial derivative of the limiting current is given by

$$\partial \ln i_L/\partial x = -\partial \ln \delta(x)/\partial x \tag{7}$$

For a nearly circular (disk) deposit, of a radius r, the ohmic resistance at position x (along the radius vector of the deposit), $R_L(x)$, is given by[11]

$$R_L(x) = (\pi/2\kappa)\sqrt{r^2 - x^2} \tag{8}$$

and its derivative is

$$\partial R_L(x)/\partial x = -(\pi/2\kappa)x/\sqrt{r^2 - x^2} \tag{9}$$

Thus, near the edge of the growing deposit ($x \approx r$) the resistance vanishes and its spatial derivative along the radius vector is very large. Under these conditions the Wagner number takes on the simpler form

$$W = \frac{1}{l\{1 + [i_0/i_L(x)]\zeta(x)\}} \times \frac{\{1 + [i_0/i_L(x)]\zeta(x)\}^2 + (i_0/b)\zeta(x)\left(\frac{RT}{nF}\right)\left(1 - \frac{i}{i_L}\right)^{-1}\left(\frac{1}{i_L}\right)}{(1/b)\left(-i\frac{\partial R_L}{\partial x}\right)} \tag{10}$$

For small electric currents, or "infinite" limiting currents, so that $i/i_L \ll 1$, this expression reduces to

$$W = \frac{b}{\left(-i\frac{\partial R_L}{\partial x}\right)l} \tag{11}$$

We made use of the fact that in the Tafel region, and when mass transport is unimportant,

$$i = i_0\xi(x) = i_0 \exp\{b^{-1}[\eta(x) - i(x)R_L(x)]\}$$

Therefore

$$i/i_L = i_0\zeta(x)/i_L \ll 1$$

eq 11 is the well-known form of the Wagner number. However, at the edge of the disk, the resistance vanishes, its derivative is singular, and the Wagner number approaches zero. Thus growth at the edge is strongly favored relative to growth at some internal point on the cathode.

For electric currents approaching the mass-transport limiting values the Wagner number at the growing edge of the electrodeposit is given by

$$W = \frac{[i_0/i_L(x)]\zeta(x)b + \left(\frac{RT}{nF}\right)\left(1 - \frac{i}{i_L}\right)^{-1}}{\left[\left(\frac{RT}{nF}\right)\left(1 - \frac{i}{i_L}\right)^{-1}\left(\frac{i}{i_L}\right) + bi_0/i_L(x)\zeta(x)\right]\frac{\partial \ln i_L}{\partial x} - i\frac{\partial R_L}{\partial x}} \tag{12}$$

If we neglect the first term of the denominator with respect to the derivative of the resistance, we obtain

$$W = \frac{[i_0/i_L(x)]\zeta(x)b + \left(\frac{RT}{nF}\right)\left(1 - \frac{i}{i_L}\right)^{-1}}{-i\frac{\partial R_L}{\partial x}} \tag{13}$$

Otherwise, if the first term in the denominator of eq 12 is so large that the second can be neglected, i.e., close to mass-transport control conditions, then we find

$$W = \frac{1}{\frac{\partial \ln i_L}{\partial x}l} = -\frac{1}{\frac{\partial \ln \delta}{\partial x}l} \tag{14}$$

The form of the Wagner number close to the center of the deposit, when $x \approx 0$, is

$$W = \frac{1}{l\{1 + [i_0/i_L(x)]\zeta(x)\}} \times \frac{\{1 + [i_0/i_L(x)]\zeta(x)\}^2 + (i_0/b)\zeta(x)\left[\left(\frac{RT}{nF}\right)\left(1 - \frac{i}{i_L}\right)^{-1}\left(\frac{1}{i_L}\right) + R_L(x)\right]}{(1/b)\left\{\left[\left(\frac{RT}{nF}\right)\left(1 - \frac{i}{i_L}\right)^{-1}\left(\frac{i}{i_L}\right) + bi_0/i_L(x)\zeta(x)\right]\frac{\partial \ln i_L}{\partial x}\right\}} \quad (15)$$

This takes on the following form for currents very much smaller than the limiting current,

$$W = \frac{1 + iR_L(x)}{\left(\frac{i}{i_L}\right)\left[\left(\frac{RT}{nFb}\right) + 1\right]\frac{\partial \ln i_L}{\partial x}l} \qquad i \ll i_L \quad (16)$$

When $i \approx i_L$ eq 14 applies.

We will use these expressions to explain the experimental trends observed upon the variation of the system parameters.

B. Interfacial vs Bulk Deposition. The most fundamental question concerning electrodeposition at the liquid interface is why we observe mostly thin, quasi-two-dimensional growth parallel to the interface, rather than globular, three-dimensional growth occupying all space available to it.

Let us first consider the situation at the center of the deposit. Once a disklike structure evolves, mass transport (mostly diffusional) rapidly starts dominating the process for points close to the center of the electrode. Then eq 14 holds. There is no reason to expect, a priori, any variance in the limiting current or in the width of the diffusion layer for these near-center points. Mass transport by convection is also not expected. Hence the generalized Wagner number is expected to be large, and the growth normal to the surface will be compact. It might be rough on the scale of the thickness of the Nernst layer (typically a few micrometers). In such a case the deposit will appear black. The growth rate in the direction normal to the surface under these conditions is slow, as it is determined by slow diffusional processes. The relatively low electric field near the center also does not favor a significant contribution of ionic migration. Thus, at the center of the deposit a flat morpholgy, perhaps with some micrometer scale roughness, is the stable morphology.

By contrast, near the edge eqs 11 and 12 are valid. These equations involve the derivative of the ohmic resistance, which is singular, giving a vanishingly small Wagner number and resulting in highly unstable fronts. The edges might become ramified, as well, depending on the precise value of the Wagner number calculated for two points along the edge. The tips of the growing deposit push forward, and this growth is augmented by the spherical diffusional conditions prevailing near them (or hemicylindrical conditions near a smooth portion of the edge). This provides a positive feedback for further growth of the tips, compared to the recesses which are masked by the tips. Their motion stimulates local convection, which makes the mass transport even more efficient, and increases the electric current. Furthermore, the edge advances toward virgin regions of the solution which are not yet depleted by the reaction. This effect is especially large for very thin deposits that require a small amount of deposition in order to advance. All this results in fast growth of the edges. These different growth conditions at the edge of the deposit, compared to its center, are responsible for the quasi-two-dimensional patterns. Many researchers in the past indeed showed that for simple cases of primary current distributions, the edges exhibit significantly larger electric currents than more centrally located points.[9]

When the intrinsic electrochemical reaction is slowed (by poor wetting of the deposit,[4] for instance) the deposit will take on intermediate forms between highly ramified 2D patterns and compact 3D shapes, such as 2D disks or "flowers". When the electrodic reaction becomes exceedingly slow, as in the presence of poisons,[5] the growth becomes fully three-dimensional.

This analysis explains why a planar formation might form at all. However, it apparently should apply to a bulk situation as well, where we do not get flat, thin deposits, but rather three-dimensional ones. Furthermore, it does not explain why at the interface the 2D deposits develop only parallel to the interface and not just in any direction. In fact, in the absence of the surfactant we found it difficult to obtain a 2D deposit at all, unless one micropositions the tip of the cathode with great care to merely touch the interface.[4,5] We believe that the role of the interface is to force quasiplanar mass transport, at the very early stages of the deposition. Thus, a definite orientation of a planar growth is "seeded" in the surface-parallel orientation. Once this "seed"-deposit forms, the Wagner mechanisms discussed above take over and propagate the instability parallel to the interface. These mechanisms also determine the degree of ramification within the deposit. Even this initial induction by the interface is often not strong enough, and a 3D nucleus-deposit may be obtained. Once it forms, it continues to grow in three dimensions utilizing the spherical or hemispherical diffusional conditions. The fact that in our system we obtain, nevertheless, mostly 2D, surface-parallel growth highlights the importance of the surfactant as a stabilizing agent for such growth, as we discuss below. In the bulk (like when the tip of the electrode protrudes into the solution) none of the mechanisms we discussed above are effective in forming a flat precursor and the Wagner amplification does not take place.

C. Dependence of the Morphology on the Electric Potential. The morphology is dictated by the Wagner numbers at the edge, given by eqs 10, 12, 13. The denominator of eq 11 increases exponentially with the overvoltage (in the Tafel region). Thus, when the currents are smaller than the limiting currents, the Wagner number decreases monotonically with the voltage. The exponential dependence is weakened by the IR potential drop, which also increases with the overall voltage. In any event, in this limit the Wagner number should become smaller with increasing potential, and the deposits should become increasingly ramified. The electric currents should, of course, increase as well, and the time duration of the growth to a given size should decrease. Both of these phenomena are observed for the relatively low conductivity of the standard sample, where the silver nitrate is expected to exhibit drift (motion in an electric field), in addition to diffusion, giving high effective limiting currents. At high voltages (above 5−6 V) hydrogen evolution slows down the processes, causing lower growth rates and more compact shapes.

When the system approaches the mass-transport-dominated regime, the limiting eq 13 or 14 holds. In eq 13 the denominator becomes independent of the voltage ($i = i_L$), while the numerator increases with it. Thus, in this limit, larger overvoltages result in larger Wagner numbers and in more compact deposits (2D or even in extreme cases 3D). Equation 14 yields large Wagner numbers on any scale larger than the width of the Nernst diffusion layer. Therefore it too predicts smoother deposits at high potentials (and ionic strength) at the resolution of our experiment (hundreds of micrometers). Indeed, at higher ionic strengths obtained by adding an inert electrolyte (ammonium nitrate), the limiting current is determined only by the slow silver ion diffusion. Our results show that the deposits become progressively compact as the overvoltage increases, in agreement with eq 13 or 14. The currents are lower due to the setting in of the slow diffusion (and the weaker convection), and the deposition time therefore should increase, as is indeed observed.

D. Dependence of the Morphology on the Conductivity. As the conductivity increases, at fixed silver ion concentration, and constant overall voltage, the denominators of eqs 11 and 13 decrease. Also the contribution to the current from the silver ions' drift becomes less important, as the current is carried predominately by the inert electrolyte. The mass transport of silver ions becomes slower and is translated into a lower limiting current. Note that we loosely use the term limiting current incorporating also any contribution from migration of silver ions to the transport near the electrode. In addition, the IR drop becomes smaller, so that a larger fraction of the applied voltage actually falls on the electrode/electrolyte interface and drives the electrodic reaction. The net outcome of this situation is a transition of the Wagner number from a small value given by eq 11 to a large value that is given by eq 12 and its limiting forms eqs 13 and 14. In eq 13 the denominator gradually decreases as the conductivity increases (see eq 9), and the numerator increases, with $\zeta(x)$ increasing exponentially (eq 5) and i approaching i_L. Equation 14 gives large Wagner numbers on scales very much larger than that of the diffusion layer.

Consequently, the deposits should become progressively compact as the ionic strength increases. This is the trend we observe in the experiments presented here. The same conclusion is reached based on the simple form of the Wagner number,[8,9] which is essentially eq 11. With increasing ionic strength the resistance of the solution decreases and the system becomes chemically controlled, rather than exhibiting a primary current distribution.

On the basis of these considerations the growth rate of the 2D deposit should decrease when the ionic strength increases. The overall electric current can still increase as the IR drop becomes smaller and there is progressively more pronounced hydrogen evolution. This side reaction uses up some of the current and also slows down the deposition by (partly) blocking the electrode surface.

E. Dependence of the Morphology on the Concentration of Silver Ions (Constant Ionic Strength). As the concentration of the silver ions increases, the limiting current increases and so does the exchange current. Thus, the numerator of eq 12 hardly changes, while that of eq 11 depends on the Tafel slop alone. On the other hand, the denominators of both equations increase, giving smaller Wagner numbers, regardless of which equation is valid. Consequently, we predict a transition from compact to ramified structures when the concentration is increased. This trend, though weak, is indeed observed, as pointed out above in the discussion of Figure 11.

F. Dependence of the Morphology on the Concentration of Silver Ions (Varying Ionic Strength). In this series of experiments the situation is more complex. Both the currents and the resistance of the solution change; the former increases and the latter decreases with increasing silver ion concentration. However, the electric current changes much faster, as, in addition to its *linear* dependence on the concentration (through the exchange current density i_0 and/or the limiting current density i_L), it manifests an *exponential* dependence on the IR drop, which, in turn, is affected by the ionic strength. Therefore, we expect that as long as there is a considerable IR drop across the solution, the denominator of eq 11 will increase with increasing concentration, resulting in a shift to more ramified deposits. This is what is observed in our experiments. Recall that the growth along the interface in the standard sample is not at its mass-controlled limit, as evidenced, for instance, from the dependence of the deposition time on the voltage. At high ionic strengths, when the IR drop is small, the current and the resistance change similarly with the concentration (both are proportional to it). Furthermore, hydrogen evolution sets in, slowing down all the deposition processes and resulting in more compact forms.

G. Dependence on the Viscosity. Increasing the viscosity of the aqueous subphase results in a proportional decrease in the diffusion coefficients and the mobilities of the ions. Also convection is retarded. Thus the mass-transport limiting current decreases, while the resistance increases. At the more central areas of the growing deposit, which presumably were under mass-transport control, the current should now decrease in direct proportion to the increase in viscosity. At the edges, too, mass-transport can become more important than under the standard conditions. Thus, it is expected that the total currents will decrease approximately linearly with the viscosity, as is, indeed, observed (see Figure 12b).

Due to the setting-in of some mass-transport control at the edges, the rate of growth (parallel to the surface) is also expected to decrease, as the viscosity increases. This, too, has been observed.

In eq 11 the product of the current and the resistance determine the value of the Wagner number. When the viscosity increases, the resistance also increases, and the total current and the growth rate (indicative of the current at the edge) decrease, proportionally. Thus, we would expect the product of the resistance and the current to remain nearly constant, and, by eq 11, we would not expect any morphological changes. However, we do observe an increase in the ramification of the edge of the deposit when the viscosity increases. Apparently, mass transport to the edge attains some importance, and the full eq 4 should be used instead of eq 11. A decreasing limiting current in eq 4 can give larger values of the generalized Wagner number, provided that the second term in the denominator becomes the dominant term. The observation that the growth rate is, in fact, affected by the viscosity is additional evidence that mass transport becomes important as the viscosity increases.

H. Role of the Surfactant. We mentioned above that at the concentrations we use the surfactant does not have any significant effect on the shape of the deposit or its rate of formation. It only renders the deposit a little more compact and/or its branches a little broader. It, however, improved the reproducibility of the experiments considerably. In a previous study[4] we showed that at a much higher surfactant concentration (30-fold higher than that used here) the deposits become considerably more compact. This was explained on the basis of a change in the wetting of the advancing electrodeposit by the aqueous environment. At the low concentration of our present study, this effect is negligible. Instead, it seems that the surfactant promotes the initial growth parallel to the surface. Once that thin, surface-parallel, "seed"-deposit is formed, it will induce, under most conditions a thin, surface-parallel growth of the deposit, as discussed above. It is plausible that the surfactant, as it preferentially segregates at the interface, carries with it also silver ions. Indeed, we have shown[12] that a surfactant−silver ion layer really forms at the interface. This (partial) monolayer can supply the initial quantity of ions needed to form a "seed"-deposit along the interface. In their study of silver monoparticulate films Fendler et al.[3a,b] demonstrated the great sensitivity of the electrocrystallization, to the nature of the surfactant. Anionic surfactants that attract silver ions induced surface electrocrystalization while cationic surfactants did not. They and Tai et al.[3c] showed also a definite dependence of the process on the precise surface pressure. However, we stress that still most of the ions required for the growth must come from the solution itself.

I. Numerical Estimates. The discussion above indicates that an analysis based on the generalized Wagner number can, indeed, account well for all our observations at the qualitative level. Let us examine now some of the quantitative implications, starting from the standard experimental conditions.

For $x = r - l$ we obtain from eq 11

$$W = \frac{2\kappa b}{i\pi\sqrt{r/2l}} \tag{17}$$

We carry out our estimate for a deposit halfway to the cell wall, i.e. a radius of ~1.5 cm and an area of ~7 cm^2. The specific conductivity of a 0.05 M $AgNO_3$ solution is $\sim 7.7 \times 10^{-3}$ Ω^{-1} cm^{-1}.[13] The Tafel slope of silver (divided by 2.3) is $b = 0.05$ V.[14] From the results of Figure 3 the overall electric current at −5 V, for a deposit halfway to the cell wall, is about 0.13 A. Assuming a uniform distribution over the electrode area yields a current density of ~0.02 A/cm^2. This, of course, is an approximation, as only part of the current flows through the edges, taken here as 0.1 cm wide. Inserting these values into eq 17 yields a Wagner number of ~0.004. This is a small value indeed, and a ramified deposit is expected. We take this value as a reference point and estimate on its basis the Wagner number at lower voltages. An actual decrease of 0.5 V in the overvoltage makes the electric current about 10^{-10}-fold smaller. Thus one can easily go from small Wagner numbers to large values (which give compact structures) by changing the potential very slightly. In fact, even if the edge current density for the standard conditions is much higher than we estimated, as the thickness of the edge is very small, we reach the same conclusion: at −5 V the deposit should be ramified, while at lower potentials it should become compact. As an extreme example, if we suppose that the entire electric current flows through the edge of thickness 20 nm, the Wagner number at −5 V is $\sim 1 \times 10^{-8}$, while at a −4.5 V it is ~100. Thus, these simple numerical estimates agree surprisingly well with the experimental findings. One should note that 2−3 V out of the 5 V total drop are merely an IR drop across the cell. Therefore, when the nominal voltage changes from −5 V to −4 V, for example, the actual overvoltage changes by a much smaller degree, say by about 0.3−0.4 V only.

As another example consider changing the ionic strength at a constant overall voltage and silver ion concentration, from 0.05 M to 0.154 M, by adding ammonium nitrate. The motion of the silver ions has now a much weaker drift component, and it is mostly governed by the slow diffusion. Equation 13 is now valid. Of the two expressions in the numerator the first one is the Tafel slope multiplied by a large number, while the numerator in eq 11, supposedly holding for the standard conditions, is only the Tafel slope. The reduced IR drop is expressed exponentially in the expression for $\zeta(x)$ and makes it grow substantially. We saw above that typically a 0.5 V change makes a 10^{10}-fold effect. The current density, i, in the denominator is limited to i_L or lower. The net effect is an increase of the Wagner number by many orders of magnitude, to values far above unity. Thus, the change to compact structures, observed experimentally when the conductivity is increased, is clearly accounted for.

Experimentally, we note that as the ionic strength increases, hydrogen evolution becomes increasingly important. This has the effect of disturbing the deposition reaction by (partly) blocking the access of the ions to the electrode surface. Hence, neglecting convection, the effective exchange current for the deposition should decrease and the Wagner number will increase. We see that the onset of hydrogen evolution acts in the same direction as the effects stemming from the onset of mass-transport control we discussed above. Except at the lower potentials, or ionic strengths, it is impossible to distinguish between these different effects.

Summary

We presented a systematic study of silver electrodeposition at the water/air and the water/DCM interfaces. Qualitatively, the behavior in both interfaces is similar, although there are quantitative differences in the morphology of the deposits, the rates of their formation, and their precise dependence on the various system control parameters. We interpret the results in terms of a generalized Wagner number and its dependence on voltage, conductivity, silver ion concentration, viscosity, etc.

Acknowledgment. This work was carried out with partial support of the Israel Science Foundation founded by the Israel Academy of Sciences and Humanities.

References and Notes

(1) Bockris, J. O'M.; Reddy, A. K. N. *Modern Electrochemistry*; Plenum Rosseta: 1973; p 1173.

(2) (a) Garik, P.; Barkey, D.; Ben-Jacob, E.; Bochner, E.; Broxholm, N.; Miller, B.; Orr, B.; Zamir, R. *Phys. Rev. Lett.* **1989**, *62*, 2703. (b) Sawada, Y.; Dougherty, A.; Gollub, J. P. *Phys. Rev. Lett.* **1986**, *56*, 1260. (c) Matsushita, M.; Sano, M.; Hayakawa, Y.; Honjo, H.; Sawada, Y. *Phys. Rev. Lett.* **1984**, *53*, 286. (d) Melrose, J. R.; Hibbert, D. B.; Ball, R. C. *Phys. Rev. Lett.* **1990**, *65*, 3009. (e) Fleury, V.; Chazalviel, J. N.; Rosso, M. *Phys. Rev. Lett.* **1992**, *68*, 2492.

(3) (a) Zhao, X. K; Fendler, J. H. *J. Phys. Chem.* **1990**, *94*, 3384. (b) Kotov, N. A.; Zaniquelli, M. E. D.; Meldrum, F. C.; Fendler, J. H. *Langmuir* **1993**, *9*, 3710. (c) Tai, Z.; Zhang, G.; Qian, X.; Xiao, S.; Lu, Z.; Wei, Y. *Langmuir* **1993**, *9*, 1601.

(4) Zeiri, L.; Efrima, S.; Deutsch, M. *Langmuir* **1996**, *12*, 5180.

(5) Younes, O.; Zeiri, L.; Efrima, S.; Deutsch, M. *Langmuir* **1997**, *13*, 1767.

(6) Efrima, S. *Langmuir* **1997**, *13*, 3550.

(7) Zeiri, L.; Efrima, S.; Deutsch, M. *Phys. Rev. Lett.*, accepted for publication.

(8) Wagner, C. *J. Electrochem. Soc.* **1954**, *101*, 225.

(9) Ibl, N. In *Comprehensive Treatise of Electrochemistry*; Yeager, E., Bockris, J. O'M., Conway, B. E., Sarangapani, S., Eds.; Plenum Press: New York, 1983; Vol. 6, p 239.

(10) (a) Barkey, D.; Garik, P.; Ben-Jacob, E.; Miller, B.; Orr, B. *J. Electrochem. Soc.* **1992**, *139*, 1044. (b) Barkey, D. P.; Muller, R. H.; Tobias, C. W. *J. Electrochem. Soc.* **1989**, *136*, 2207. (c) Landau, U. *Proc. Electrochem. Soc.* **1994**, *94*−*22*, 77.

(11) Newman, J. *J. Electrochem. Soc.* **1966**, *113*, 501.

(12) Gorodinski, E.; Efrima, S. *Langmuir* **1994**, *10*, 2151.

(13) *CRC Handbook of Chemistry and Physics*, 73rd ed.; CRC: Boca Raton, 1992−1993; pp 5−110.

(14) Shumilova, N. A.; Zhutaeva G. V. In *Encyclopedia of Electrochemistry of Elements*; Bard, A. J., Eds.; Marcel Dekker: New York, 1973; Vol. 8, p 1.